

An energy solution to the shear deformation of corrugated plates

Autor(en): **Horne, M.R. / Raslan, R.A.S.**

Objekttyp: **Article**

Zeitschrift: **IABSE publications = Mémoires AIPC = IVBH Abhandlungen**

Band (Jahr): **31 (1971)**

PDF erstellt am: **28.05.2024**

Persistenter Link: <https://doi.org/10.5169/seals-24208>

Nutzungsbedingungen

Die ETH-Bibliothek ist Anbieterin der digitalisierten Zeitschriften. Sie besitzt keine Urheberrechte an den Inhalten der Zeitschriften. Die Rechte liegen in der Regel bei den Herausgebern.

Die auf der Plattform e-periodica veröffentlichten Dokumente stehen für nicht-kommerzielle Zwecke in Lehre und Forschung sowie für die private Nutzung frei zur Verfügung. Einzelne Dateien oder Ausdrucke aus diesem Angebot können zusammen mit diesen Nutzungsbedingungen und den korrekten Herkunftsbezeichnungen weitergegeben werden.

Das Veröffentlichen von Bildern in Print- und Online-Publikationen ist nur mit vorheriger Genehmigung der Rechteinhaber erlaubt. Die systematische Speicherung von Teilen des elektronischen Angebots auf anderen Servern bedarf ebenfalls des schriftlichen Einverständnisses der Rechteinhaber.

Haftungsausschluss

Alle Angaben erfolgen ohne Gewähr für Vollständigkeit oder Richtigkeit. Es wird keine Haftung übernommen für Schäden durch die Verwendung von Informationen aus diesem Online-Angebot oder durch das Fehlen von Informationen. Dies gilt auch für Inhalte Dritter, die über dieses Angebot zugänglich sind.

An Energy Solution to the Shear Deformation of Corrugated Plates

Solution par l'énergie pour les déformations de cisaillement de tôles

Eine Energielösung für die Schubverformung gerippter Bleche

M. R. HORNE

M. A., M. Sc., Ph. D., Sc. D.
Professor of Civil Engineering

R. A. S. RASLAN

B. Sc., Ph. D.

University of Manchester, England

1. Introduction

The stiffness and general behaviour of corrugated plate shear panels, Fig. 1, has been extensively investigated because of the capability of such panels to withstand considerably larger shear loads without overall buckling as compared with plane plate shear panels.

Such panels are usually attached to the supporting frame along the bottom plate of each corrugation, implying that the shear forces R are applied in the plane of the bottom plates and not in the plane of the shear centres of the corrugations. This eccentricity causes the corrugations to deform with a twisting component as shown at a typical cross-section in Fig. 2a.

Thus, a generating line along the corrugation length (length will always denote the dimension parallel to the corrugations) will not remain straight and parallel to its original position when deformed as in the case of plane plates, but will twist in plan about its mid-point. The twisted shape of the line will depend on the boundary conditions at its ends. A line AA at the mid-width of the top plate will twist to position $A'A'$ as shown by Fig. 4a, while a line HH at the mid-width of the bottom plate will have the shape $H'H'$ as shown by Fig. 4c. A line KK at the mid-point of a side plate deforms into $K'K'$ as shown by Fig. 4b.

The twisting of the corrugation cross-section, Fig. 2a, is associated with plate bending stresses, with the notation of Fig. 5b, the coordinate direction y being parallel to the corrugations (Fig. 1). The deformation of the generating lines

AA , HH and KK , Fig. 4, is associated with plate membrane stresses with the notation of Fig. 5a.

Theoretical solutions have been obtained for trapezoidal [1, 2] and semi-circular [5] corrugations. These solutions are based on the following assumptions: a) line AA , Fig. 4a, remains straight after deformation; b) line HH , Fig. 4c, does not deform and remains parallel to its original position and c) the stresses which develop in the middle surface of the plate are, referring to Fig. 5, τ_{xy} , τ_{yx} and M_y only. It is shown in the present paper that these assumptions lead to an overestimate of the stiffness of the panel. LUTTREL [4] retains assumptions (b) and (c) but allows for the fact that lines AA do not remain straight after deformation. He finds the deformation of these generating lines to be localised within two regions at the ends of the corrugations, extending into the panel to a certain length, after which lines AA remain parallel to their original positions. Within the central region as defined, stresses τ_{xy} and τ_{yx} only exist. Luttrell describes the deformed shape of lines AA as a parabola of the n th degree where n depends on the panel configuration and the spacing of the end fasteners. The value of n is obtained experimentally.

The method of solution, presented in the present paper, assumes in-plane deformation patterns for each of the three plates which form a trapezoidal corrugation, that is, the top, bottom and two side plates. A general energy term is then developed and minimized with respect to the coefficients that exist in the assumed deformation patterns. The deformed shape and the shear stiffness of a corrugation or a corrugated panel can then be obtained.

2. Definition of Problem

The corrugations consist of top plates of width $2b_T$, bottom plates of width $2b_B$ and side plates of symmetrical inclination θ as shown in Fig. 2a. The depth of the corrugations is d and the total length is $2a$ (Fig. 1). When the panel of Fig. 1 is shear loaded, a cross section within the length of an intermediate corrugation (the dotted line $E'B'C'D'E'B'$ as shown by Fig. 1) will twist to a position $EBCDEB$ as shown by Fig. 2a. The displacements of the corrugation corners $BCDE$ could be defined with respect to either set of components, u_S (in the plane of the side plate) and p_T (or p_B) (perpendicular to u_S) or u_T (or u_B) (in the plane of the top or bottom plate) and v_T (or v_B) (perpendicular to u_T or u_B) as shown by Fig. 2b.

Bending stresses (M_y in Fig. 5b) will develop, these being associated with out of plane deflections w_T , w_S and w_B for the top, side and bottom plate respectively as shown in Fig. 2a. These bending stresses will be assumed to have linear distributions between the corner moments (M_E , M_B , M_C and M_D in Fig. 2a). This type of bending will be referred to as "portal frame bending".

The twisting of a cross section $IFG'J'IF$ at the end of the corrugation

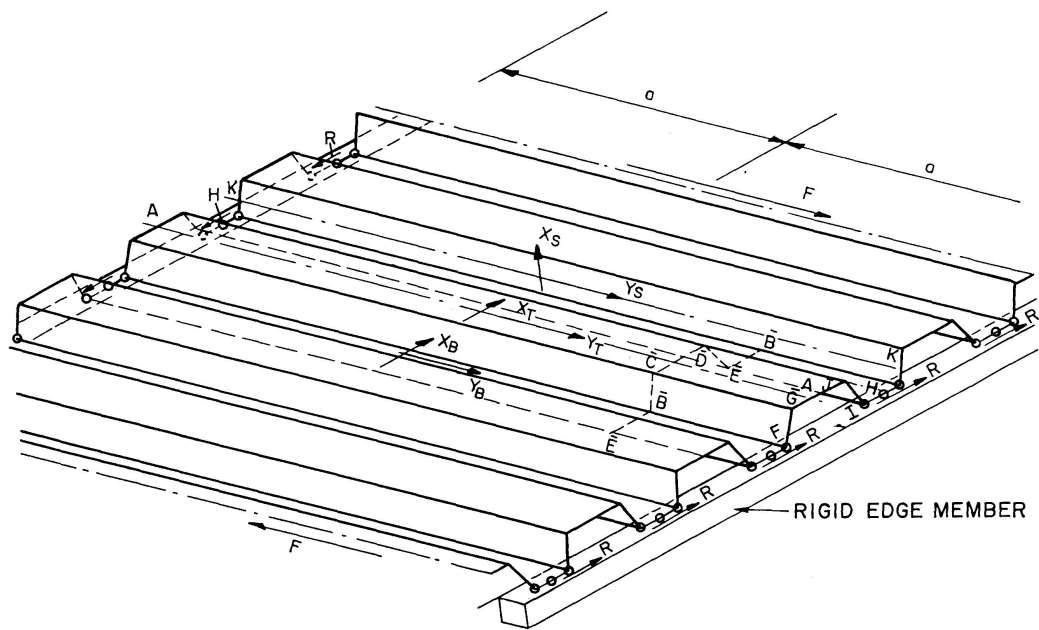


Fig. 1.

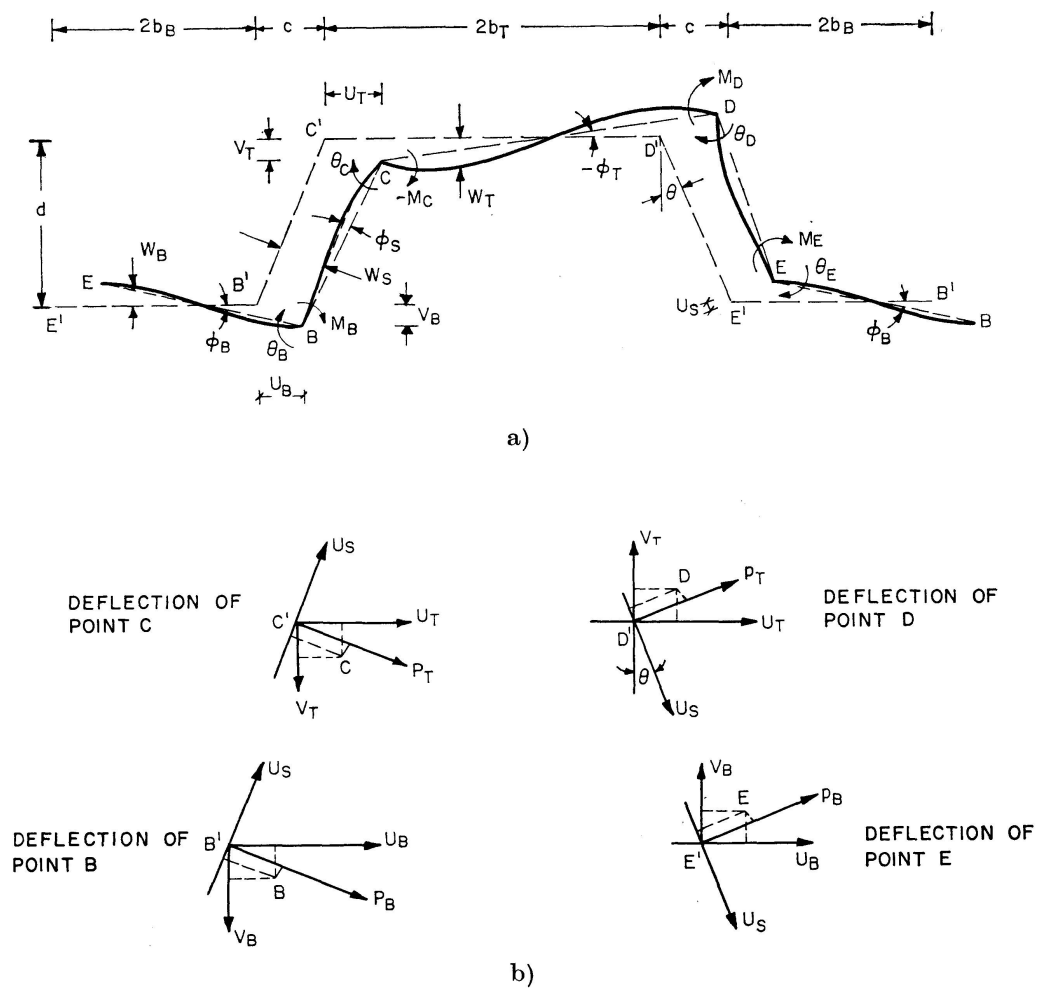


Fig. 2.

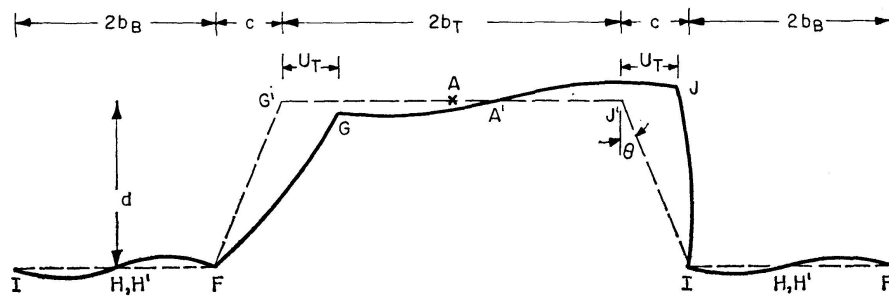


Fig. 3. Portal Frame Deformations at End of Panel.

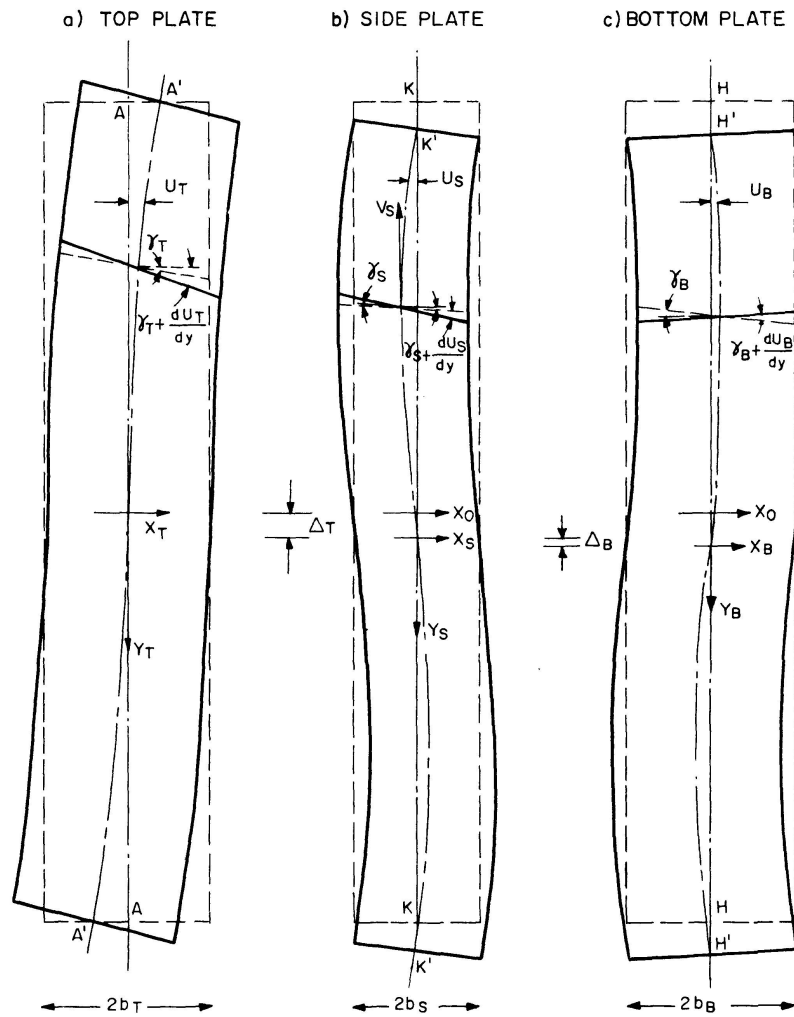


Fig. 4. Deformation of Plates in Their Planes.

(Fig. 3) will be more restricted due to the boundary conditions. Points H (being the locations of the plate to frame fasteners) are fixed in the X -direction and in the present solution will be assumed to be fixed in a direction perpendicular to the bottom plate.

Due to the difference in the modes of twist between cross sections within the length (Fig. 2a) and those at the ends of the corrugation (Fig. 3), the top, side and bottom plates will adopt the shapes shown by Fig. 4, with in-plane

deflection functions u_T (with maximum values at the ends), u_S and u_B (with zero values at the ends) for the top, side and bottom plate respectively. By symmetry, u_T , u_S and u_B will be zero at the mid-length of the corrugations. Assuming the top, bottom and side plates to be long compared with their width, these deflections may be regarded as the deflections of the central axes of these plates considered as "beams" bent in their own planes. The membrane stresses σ_y (Fig. 5a) are then the "bending stresses" of these prismatic "beams", and as in the usual Bernoulli theory of bending may be assumed to vary linearly between the edges of the plates.

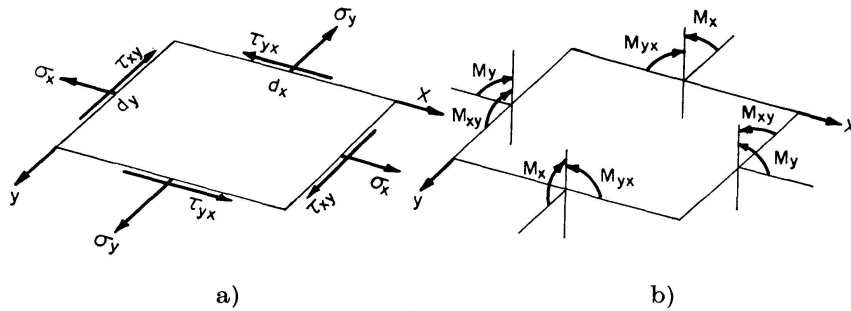


Fig. 5.

Because of the difference in the in-plane deflection functions of the different plates and the existence of the membrane shear stresses (τ_{xy} and τ_{yx} in Fig. 5a), shear strains γ_T , γ_S and γ_B take place in the top, side and bottom plates (Fig. 4). Finally because of the different "beam bending strains" existing at the edges of the top and bottom plates, the side plates will, in addition to linearly varying "beam bending stresses" σ_y , also contain an additional mean longitudinal stress σ_y , with which will be associated an extension function v_S in the Y direction as indicated in Fig. 4b. Such extension functions will not occur in either the top or bottom plates, as may be seen by reversing the direction of the overall shear force acting on the panel.

Non-linear membrane stresses σ_y will be induced at large angles of twist (reference [2]). These are however of significance only for very short panels and will be ignored. Membrane stresses σ_x (Fig. 5a) will be neglected because of the considerable flexibility of the corrugations in this direction. The strain energy due to bending stresses M_x , and twisting stresses M_{xy} , M_{yx} (Fig. 5b) will be neglected because of the very small value of $\frac{\partial^2 w}{\partial x^2}$ and $\frac{\partial^2 w}{\partial x \partial y}$ compared with $\frac{\partial^2 w}{\partial y^2}$. Confirmation of the small size of energy terms associated with twisting stresses M_{xy} has been obtained by considering the twisting of the top, bottom and side plates treated as prismatic beams [6].

Equilibrium equations relating all the effective stresses of Fig. 5 have been developed and solved [6, 7]. The present paper is devoted to describing the energy solution, the results of which will be compared with the equilibrium solution.

3. Assumptions and Limitations

These are as follows.

1. The material is infinitely elastic.
2. The marginal frame is a hinged parallelogram consisting of rigid members.
3. The plate is pinned to the frame at the mid-width of each end of each bottom plate, the end corners of each bottom plate (points F and I in Fig. 3) being prevented from up lifting.
4. No slip takes place due to bearing between the plate and the fasteners.
5. No overall buckling occurs.
6. The panel is very wide, consisting of a large number of corrugations, so that the effect of any particular boundary conditions on the end corrugations may be neglected.
7. The effect of large deformations is neglected.

4. Method of Solution

The method is to assume modes of deformations for each of the individual plates (top, side and bottom plate). These should satisfy the boundary conditions, the compatibility condition implied by the integrated behaviour of the plates and any conditions of symmetry or anti-symmetry. The energy terms due to the assumed deformations are then obtained and the total strain energy in one corrugation is obtained after minimizing it with respect to each of the parameters which appear in the assumed modes of deformation. The internal strain energy is lastly equated with the work done by the applied loads to obtain the load corresponding to the deformation state.

In calculating the total strain energy, the following terms are introduced:

1. Due to bending stresses:

U_1 is the strain energy due to the plate bending stresses M_y (Fig. 3).

2. Due to membrane stresses:

U_2 is the strain energy due to that part of the stresses σ_y (Fig. 3) which cause the extension v_s in the side plates (Fig. 4b).

U_3 is the strain energy due to the linearly varying stresses σ_y in the top plate associated with its bending as a "beam" in its own plane.

U_4 is the strain energy due to the linearly varying stresses σ_y in the bottom plate.

U_5 is the strain energy due to the linearly varying stresses σ_y in the side plates.

U_6 is the strain energy due to shear strains γ_T in the top plate.

U_7 is the strain energy due to shear strains γ_B in the bottom plate.

U_8 is the strain energy due to shear strains γ_S in the side plates.

5. Modes of Deformation

Denotong by u_T , u_B and u_S the in-plane deflection of the centre lines of the top, bottom and side plate respectively at any point along OY (Fig. 4), expressions for these deflections, consistent with the boundary conditions will be assumed as follows,

$$u_T = c_0 y + c_1 \frac{a}{\pi} \sin \frac{\pi y}{a}, \quad (1)$$

$$u_B = c_2 \frac{a}{\pi} \sin \frac{\pi y}{a}, \quad (2)$$

$$u_S = c_3 \frac{a}{\pi} \sin \frac{\pi y}{a}, \quad (3)$$

where c_0 , c_1 , c_2 and c_3 are constant coefficients and a is half the panel length.

The shear strains γ_T , γ_B and γ_S at any point along OY will be assumed as:

$$\gamma_T = \alpha_0 + \alpha_1 \cos \frac{\pi y}{a}, \quad (4)$$

$$\gamma_B = \alpha_2 + \alpha_3 \cos \frac{\pi y}{a}, \quad (5)$$

$$\gamma_S = \alpha_4 + \alpha_5 \cos \frac{\pi y}{a} \quad (6)$$

and the extension of the side plate in direction OY as

$$v_S = e \left(1 - \cos \frac{\pi y}{a} \right), \quad (7)$$

where α_0 , α_1 , α_2 , α_3 , α_4 , α_5 and e are constant for a particular corrugation.

6. Energy due to Plate Bending Stresses

Referring to Fig. 2a, let b_T , b_B and b_S be half the width of the top, bottom and side plates respectively; ϕ_T , ϕ_B and ϕ_S the clockwise chord rotation of the top, bottom and side plates; θ_E , θ_B , θ_C and θ_D the clockwise rotations at points E , B , C and D respectively and M_B , M_C , M_D and M_E the clockwise moments acting on EB , BC , CD and DE respectively at points B , C , D and E . Let d be the depth of the corrugation, c the projection of the side plate width on the horizontal and t the uniform thickness of the plate.

Assuming I and F as fixed points (Fig. 3) and making use of the symmetry of deformation about axes OY through the mid-width of the top and bottom plate, the following relation exists:

$$b_B \phi_B + c \phi_S + b_T \phi_T = 0. \quad (8)$$

Introducing the term:

$$c \phi_e = b_B \phi_B - b_T \phi_T \quad (9)$$

and solving Eqs. (8) and (9) for ϕ_B and ϕ_T ,

$$\phi_B = \frac{c}{2b_B} (\phi_e - \phi_S) \quad \text{and} \quad \phi_T = -\frac{c}{2b_T} (\phi_e + \phi_S).$$

Assuming a unit length along OY , the following slope-deflection relations for the "portal frame bending" of the corrugations may be written:

$$\begin{aligned} \theta_B &= \frac{b_B}{3D} (2M_B + M_E) + \phi_B = \frac{b_S}{3D} (-2M_B - M_C) + \phi_T, \\ \theta_C &= \frac{b_S}{3D} (2M_C + M_B) + \phi_S = \frac{b_T}{3D} (-2M_C - M_D) + \phi_T, \\ \theta_D &= \frac{b_T}{3D} (2M_D + M_C) + \phi_T = \frac{b_S}{3D} (-2M_D - M_E) + \phi_S, \\ \theta_E &= \frac{b_S}{3D} (2M_E + M_D) + \phi_S = \frac{b_B}{3D} (-2M_E - M_B) + \phi_B, \end{aligned} \quad (10)$$

where $D = \frac{Et^3}{12(1-\mu^2)}$ is the flexural rigidity of the plate, E being Young's modulus and μ Poisson's ratio.

Due to symmetry of deformations $M_E = -M_B$ and $M_D = -M_C$ and hence by rearranging Eqs. (10).

$$(b_B + 2b_S) M_B + b_S M_C = 3D \left(\frac{2b_B + c}{2b_B} \phi_S - \frac{c}{2b_B} \phi_e \right), \quad (11)$$

$$b_S M_B + (b_T + 2b_S) M_C = -3D \left(\frac{2b_T + c}{2b_T} \phi_S + \frac{c}{2b_T} \phi_e \right). \quad (12)$$

The quantities ϕ_S and ϕ_e may be expressed in terms of the in-plane deflections u_T , u_B and u_S by considering components of deflections at points B and C (Fig. 2b).

Resolving at point B along the side plate:

$$u_S = u_B \sin \theta - v_B \cos \theta = u_B \sin \theta - \phi_B b_B \cos \theta \quad (13)$$

and at point C :

$$u_S = u_T \sin \theta - v_T \cos \theta = u_T \sin \theta + \phi_T b_T \cos \theta. \quad (14)$$

Resolving perpendicular to the side plate; at point B :

$$p_B = u_B \cos \theta + v_B \sin \theta \quad (15)$$

and at point C :

$$p_T = u_T \cos \theta + v_T \sin \theta. \quad (16)$$

Since

$$\phi_S = \frac{p_T - p_B}{2b_S}, \quad (17)$$

then from Eqs. (13) through (16):

$$\phi_S = \frac{u_T - u_B}{d}, \quad (18)$$

$$\phi_T = -\frac{u_T \tan \theta - u_S \sec \theta}{b_T}, \quad (19)$$

$$\phi_B = \frac{u_B \tan \theta - u_S \sec \theta}{b_B}. \quad (20)$$

Substituting from (19) and (20) into (9):

$$\phi_e = \frac{u_T + u_B}{d} - 2u_S \frac{2b_S}{dc}, \quad (21)$$

whence, substituting for ϕ_S and ϕ_e into (11) and (12):

$$M_B = \frac{D}{b_S^2 F} [J(u_T - u_B) + G u_S - G_1(u_T + u_B)], \quad (22)$$

$$M_C = \frac{-D}{b_S^2 F} [K(u_T - u_B) - H u_S + H_1(u_T + u_B)], \quad (23)$$

where:

$$\begin{aligned} F &= \frac{\left(2 + \frac{b_B}{b_S}\right)\left(2 + \frac{b_T}{b_S}\right) - 1}{3}, \\ J &= \frac{b_S}{d} \left[3 + \frac{b_T}{b_S} + \frac{c}{2b_S} \left(\frac{2b_S + b_T}{b_B} + \frac{b_S}{b_T}\right)\right], \\ K &= \frac{b_S}{d} \left[3 + \frac{b_B}{b_S} + \frac{c}{2b_S} \left(\frac{2b_S + b_B}{b_T} + \frac{b_S}{b_B}\right)\right], \\ G &= \frac{2b_S}{d} \left[\frac{2b_S + b_T}{b_B} - \frac{b_S}{b_T}\right], \\ H &= \frac{2b_S}{d} \left[\frac{2b_S + b_B}{b_T} - \frac{b_S}{b_B}\right], \\ G_1 &= \frac{c}{2d} \left[\frac{2b_S + b_T}{b_B} - \frac{b_S}{b_T}\right], \\ H_1 &= \frac{c}{2d} \left[\frac{2b_S + b_B}{b_T} - \frac{b_S}{b_B}\right]. \end{aligned} \quad (24)$$

The energy per corrugation due to "portal frame bending" is:

$$U_1 = 2 \int_0^a \left[\frac{1}{2D} \int_0^s M_y^2 ds \right] dy,$$

where the bending stresses M_y about axes y (Fig. 5) are assumed to vary linearly between the corner points of the corrugation and s is the length along the perimeter of the corrugation ($2b_T + 2b_B + 4b_S$). This leads to:

$$U_1 = 2 \int_0^a \frac{1}{2D} \left[\frac{4b_S}{3} (M_B^2 + M_B M_C + M_C^2) + \frac{2b_T}{3} (M_C^2) + \frac{2}{3} b_B M_B^2 \right] dy. \quad (25)$$

Substituting for M_B and M_C from Eqs. (22) and (23) into (25):

$$U_1 = \frac{2D}{3b_S^3} \int_0^a [p_1 w_1^2 + p_2 w_2^2 + p_3 w_3^2 + q_1 w_1 w_2 + q_2 w_1 w_3 + q_3 w_2 w_3] dy, \quad (26)$$

$$\text{where:} \quad w_1 = u_T - u_B, \quad w_2 = u_S, \quad w_3 = u_T + u_B \quad (27)$$

$$\begin{aligned} \text{and} \quad p_1 &= \frac{J^2 \left(2 + \frac{b_B}{b_S}\right) - 2JK + K^2 \left(2 + \frac{b_T}{b_S}\right)}{F^2}, \\ p_2 &= \frac{G^2 \left(2 + \frac{b_B}{b_S}\right) + 2HG + H^2 \left(2 + \frac{b_T}{b_S}\right)}{F^2}, \\ p_3 &= \frac{G_1^2 \left(2 + \frac{b_B}{b_S}\right) + 2G_1 H_1 + H_1^2 \left(2 + \frac{b_T}{b_S}\right)}{F^2}, \\ q_1 &= 2 \frac{JG \left(2 + \frac{b_B}{b_S}\right) + JH - GK - HK \left(2 + \frac{b_T}{b_S}\right)}{F^2}, \\ q_2 &= 2 \frac{-JG_1 \left(2 + \frac{b_B}{b_S}\right) - JH_1 + G_1 K + KH_1 \left(2 + \frac{b_T}{b_S}\right)}{F^2}, \\ q_3 &= 2 \frac{-GG_1 \left(2 + \frac{b_B}{b_S}\right) - GH_1 - G_1 H_1 - HH_1 \left(2 + \frac{b_T}{b_S}\right)}{F^2}. \end{aligned} \quad (28)$$

Substituting for u_T , u_B and u_S from Eqs. (1), (2) and (3) and integrating Eq. (26):

$$\begin{aligned} U_1 &= \frac{2Da^3}{9\pi^2 b_S^3} [p_4 (c_0^2 \pi^2 + 6c_0 c_1 + 1.5c_1^2) + 1.5p_5 c_2^2 + 1.5p_2 c_3^2 \\ &\quad + 3p_6 (2c_0 c_2 + c_1 c_2) + 1.5p_7 c_2 c_3 + 1.5p_8 (c_1 c_3 + 2c_0 c_3)], \end{aligned} \quad (29)$$

$$\begin{aligned} \text{where,} \quad p_4 &= p_1 + p_3 + q_2, & p_5 &= p_1 + p_3 - q_2, & p_6 &= p_3 - p_1, \\ p_7 &= q_3 - q_1, & p_8 &= q_1 + q_3. \end{aligned} \quad (30)$$

7. Energy due to Membrane Stresses

Energy due to extension in direction 0 Y of side plates (U_2):

If v_S is the extension function in direction 0 Y of the side plate as given by Eq. (7), then the total strain energy due to extension of a side plate is

$$\frac{1}{2} U_2 = \frac{2Et b_S}{2} \int_{-a}^a \left(\frac{dv_S}{dy} \right)^2 dy. \quad (31)$$

substituting form Eq. (7), this becomes

$$\frac{1}{2} U_2 = \pi^2 E t \left(\frac{b_S}{a} \right) a^2. \quad (32)$$

Energy due to "beam" bending of the top, bottom and side plates (U_3 , U_4 and U_5):

If u_T , u_B and u_S are the in-plane deflection functions of the top, bottom and side plate respectively, then:

$$U_3 = \frac{E t (2 b_T)^3}{24} \int_{-a}^a \left(\frac{d^2 u_T}{dy^2} \right)^2 dy, \quad (33)$$

$$U_4 = \frac{E t (2 b_B)^3}{24} \int_{-a}^a \left(\frac{d^2 u_B}{dy^2} \right)^2 dy, \quad (34)$$

$$\frac{1}{2} U_5 = \frac{E t (2 b_S)^3}{24} \int_{-a}^a \left(\frac{d^2 u_S}{dy^2} \right)^2 dy, \quad (35)$$

where $\frac{t(2b_T)^3}{12}$ represents the second moment of area of the top plate about the axis of bending and similarly for the bottom and side plates.

Substituting from Eqs. (1), (2) and (3), Eqs. (33), (34) and (35) lead to:

$$U_3 = \frac{\pi^2}{3} \left(\frac{E t b_T^3}{a} \right) c_1^2, \quad (36)$$

$$U_4 = \frac{\pi^2}{3} \left(\frac{E t b_B^3}{a} \right) c_2^2 \quad (37)$$

and
$$\frac{1}{2} U_5 = \frac{\pi^2}{3} \left(\frac{E t b_S^3}{a} \right) c_3^2. \quad (38)$$

Energy due to shear strains in the plates (U_6 , U_7 and U_8):

If γ_T , γ_B and γ_S are the shear strains in the top, bottom and side plate respectively, then:

$$U_6 = \frac{N}{2} (2 b_T t) \int_{-a}^a \gamma_T^2 dy, \quad (39)$$

$$U_7 = \frac{N}{2} (2 b_B t) \int_{-a}^a \gamma_B^2 dy, \quad (40)$$

$$\frac{1}{2} U_8 = \frac{N}{2} (2 b_S t) \int_{-a}^a \gamma_S^2 dy, \quad (41)$$

where N is the shear modulus of the plate material.

Substituting from Eqs. (4), (5) and (6) into (39), (40) and (41) and putting

$$N = \frac{E}{2(1+\mu)}$$

$$U_6 = \frac{E t a b_T}{1 + \mu} \left(\alpha_0^2 + \frac{\alpha_1^2}{2} \right), \quad (42)$$

$$U_7 = \frac{E t a b_B}{1 + \mu} \left(\alpha_2^2 + \frac{\alpha_3^2}{2} \right) \quad (43)$$

and

$$\frac{1}{2} U_8 = \frac{E t a b_S}{1 + \mu} \left(\alpha_4^2 + \frac{\alpha_5^2}{2} \right). \quad (44)$$

8. Compatibility Conditions

The condition is that the total shear displacement as between successive corrugations in direction OY should be equal to the sum of the deformations of the different plate elements in the same direction.

Referring to Fig. 4 and denoting by Δ_T the relative displacement, in direction OY , between the centre of the side plate and that of the top plate and by Δ_B the relative displacement between the centre of the side plate and that of the bottom plate, Δ_T and Δ_B may be expressed as follows:

$$\Delta_T = b_T \left(\frac{du_T}{dy} + \gamma_T \right) + b_S \left(\frac{du_S}{dy} + \gamma_S \right) + v_S$$

and

$$\Delta_B = b_B \left(\frac{du_B}{dy} + \gamma_B \right) + b_S \left(\frac{du_S}{dy} + \gamma_S \right) - v_S.$$

Substituting from Eqs. (1) through (7):

$$\begin{aligned} \Delta_T = & b_T \left(c_0 + c_1 \cos \frac{\pi y}{a} + \alpha_0 + \alpha_1 \cos \frac{\pi y}{a} \right) \\ & + b_S \left(c_3 \cos \frac{\pi y}{a} + \alpha_4 + \alpha_5 \cos \frac{\pi y}{a} \right) + e \left(1 - \cos \frac{\pi y}{a} \right) \end{aligned} \quad (45)$$

and

$$\begin{aligned} \Delta_B = & b_B \left(c_2 \cos \frac{\pi y}{a} + \alpha_2 + \alpha_3 \cos \frac{\pi y}{a} \right) \\ & + b_S \left(c_3 \cos \frac{\pi y}{a} + \alpha_4 + \alpha_5 \cos \frac{\pi y}{a} \right) - e \left(1 - \cos \frac{\pi y}{a} \right). \end{aligned} \quad (46)$$

Grouping terms which have coefficients of unity and terms which have coefficients of $\cos \frac{\pi y}{a}$ in both sides of Eqs. (45) and (46), the following relations are obtained:

$$\Delta_T = e + c_0 b_T + \alpha_0 b_T + \alpha_4 b_S, \quad (47)$$

$$0 = -e + c_1 b_T + \alpha_1 b_T + c_3 b_S + \alpha_5 b_S, \quad (48)$$

$$\Delta_B = -e + \alpha_2 b_B + \alpha_4 b_S, \quad (49)$$

$$0 = e + c_2 b_B + \alpha_3 b_B + c_3 b_S + \alpha_5 b_S. \quad (50)$$

The shear deformation per corrugation is Δ where $\Delta = 2(\Delta_T + \Delta_B)$, so by adding Eqs. (47) and (49) and rearranging:

$$c_0 = \frac{\Delta}{2b_T} - \alpha_0 - \alpha_2 \frac{b_B}{b_T} - 2\alpha_4 \frac{b_S}{b_T}. \quad (51)$$

Eqs. (48) and (50) can be written as follows:

$$\alpha_1 = \frac{e}{b_T} - c_1 - c_3 \frac{b_S}{b_T} - \alpha_5 \frac{b_S}{b_T}, \quad (52)$$

$$\alpha_3 = \frac{-e}{b_B} - c_2 - c_3 \frac{b_S}{b_B} - \alpha_5 \frac{b_S}{b_B}. \quad (53)$$

Eqs. (51) through (53) enable the parameters c_0 , α_1 and α_3 to be calculated in terms of the other unknown parameters which appear in the right hand side of the equations.

9. Solution by Minimisation of Total Strain Energy

The total strain energy of one corrugation is obtained by adding the individual terms (Eqs. (29), (32), (43), (36), (37), (38), (42), (43) and (44)) as follows:

$$U = U_1 + U_2 + U_3 + U_4 + U_5 + U_6 + U_7 + U_8. \quad (54)$$

This energy term (U) is a function of the eleven unknown coefficients – c_0 , c_1 , c_2 , c_3 , α_0 , α_1 , α_2 , α_3 , α_4 , α_5 and e , and by making use of Eqs. (51) through (53) the number of unknowns is reduced to eight. Each of the eight unknowns has a value which minimizes U . The minimisation of Eq. (54) with respect to the unknowns c_1 , c_2 , c_3 , e , α_0 , α_2 , α_4 and α_5 , results in eight simultaneous linear equations. These, together with Eqs. (51) through (53), allow the determination of the eleven deformation parameters giving rise to the shear deflection Δ per corrugation.

Eq. (54) is therefore differentiated with respect to the eight independent unknowns, the variation of the energy terms with respect to the dependent unknowns c_0 , α_1 and α_3 being allowed for by the introduction of terms $\frac{\partial c_0}{\partial \alpha_0} = -1$ (Eq. (51)) etc.

Equating the differentials to zero:

$$(6p_4m)c_0 + (3p_4m'b_T^3)c_1 + (3p_6m)c_2 + (1.5p_8m)c_3 + (m''b_T)\alpha_1 = 0, \quad (55)$$

$$(6p_6m)c_0 + (3p_6m)c_1 + (3p_5m + m'b_B^3)c_2 + (1.5p_7m)c_3 - (m''b_B)\alpha_3 = 0, \quad (56)$$

$$(3p_8m)c_0 + (1.5p_8m)c_1 + (1.5p_7m)c_2 + (3p_2m + 2m'b_S^3)c_3 - (m''b_S)\alpha_1 - (m''b_S)\alpha_3 = 0, \quad (57)$$

$$(6p_5m')e + (m'')\alpha_1 - (m'')\alpha_3 = 0, \quad (58)$$

$$(-2\pi^2p_4m)c_0 - (6p_4m)c_1 - (6p_6m)c_2 - (3p_8m)c_3 + (2b_Tm'')\alpha_0 = 0, \quad (59)$$

$$\left(-2\pi^2p_4m\frac{b_B}{b_T}\right)c_0 - \left(6p_4m\frac{b_B}{b_T}\right)c_1 - \left(6p_6m\frac{b_B}{b_T}\right)c_2 - \left(3p_8m\frac{b_B}{b_T}\right)c_3 + (2b_Bm'')\alpha_2 = 0, \quad (60)$$

$$\left(-2\pi^2 p_4 m \frac{b_S}{b_T}\right) c_0 - \left(6 p_4 m \frac{b_S}{b_T}\right) c_1 - \left(6 p_6 m \frac{b_S}{b_T}\right) c_2 - \left(3 p_8 m \frac{b_S}{b_T}\right) c_3 + (2 b_S m'') \alpha_4 = 0, \quad (61)$$

$$-\alpha_1 - \alpha_3 + 2\alpha_5 = 0, \quad (62)$$

where: $m = \frac{2 D a^3}{9 \pi^2 b_S^3}, \quad m' = \frac{2}{3} \pi^2 \left(\frac{E t}{a}\right), \quad m'' = \frac{E t a}{1 + \mu}.$

Eqs. (51), (52) and (53) can be written as:

$$c_1 + c_3 \left(\frac{b_S}{b_T}\right) - \left(\frac{1}{b_T}\right) e + \alpha_1 + \alpha_5 \left(\frac{b_S}{b_T}\right) = 0, \quad (63)$$

$$c_0 + \alpha_0 + \alpha_2 \left(\frac{b_B}{b_T}\right) + \alpha_4 \left(\frac{2 b_S}{b_T}\right) = \frac{\Delta}{2 b_T}, \quad (64)$$

$$c_2 + c_3 \left(\frac{b_S}{b_B}\right) + \left(\frac{1}{b_B}\right) e + \alpha_3 + \alpha_5 \left(\frac{b_S}{b_B}\right) = 0. \quad (65)$$

All terms between brackets in Eqs. (55) through (65) are constants for given corrugation length, configuration and material properties and these equations are sufficient to determine the unknown constants. Putting $\Delta = 1$ in Eq. (64), the equations are readily solved and the constants derived corresponding to unit deflection per corrugation. By substituting into Eq. (54) the total strain energy stored in one corrugation for a unit deflection per corrugation is then obtained.

If E_1 is the energy stored in one corrugation due to unit shear deflection per corrugation, then the energy U due to shear deflection Δ per corrugation is

$$U = E_1 \Delta^2.$$

If a shear deflection per corrugation of Δ is produced by a shear force F , then U is also given by

$$U = \frac{1}{2} F \Delta.$$

Hence

$$\Delta = \frac{F}{2 E_1}. \quad (66)$$

The shear deflection in n corrugations due to shear force is $\Delta_n = n \Delta$.

10. Modes of Deformation and Relative Importance of the Energy Terms

It is of interest to consider the influence of various factors on the behaviour of corrugated shear panels. The factors that are here considered are

1. the length of the panel,
2. the configuration of the corrugation,
3. the thickness of the plate.

The main variation in the deflected shape may be followed by considering the deflection of the centre lines of the top, side and bottom plates (u_T , u_S and u_B in Fig. 4). The relative magnitudes of the energy terms may be conveniently expressed by quoting the ratios U_i/U where U is the total energy and the U_i ($i = 1$ to 8) are the various components already defined.

1. The Effect of Panel Length

Fig. 6 shows the effect of change in length ($2a$) of the panel on the contribution of the different energy terms of Eq. (54) to the total stored energy. Note that the vertical scale ($\frac{U_i}{U}$) is logarithmic.

When the panel is short, the overwhelmingly dominant energy term is that due to "portal frame bending" (U_1). Eq. (54) is thus effectively reduced to $U = U_1$. It appears also from Fig. 11, which shows the deflections u_T , u_S and

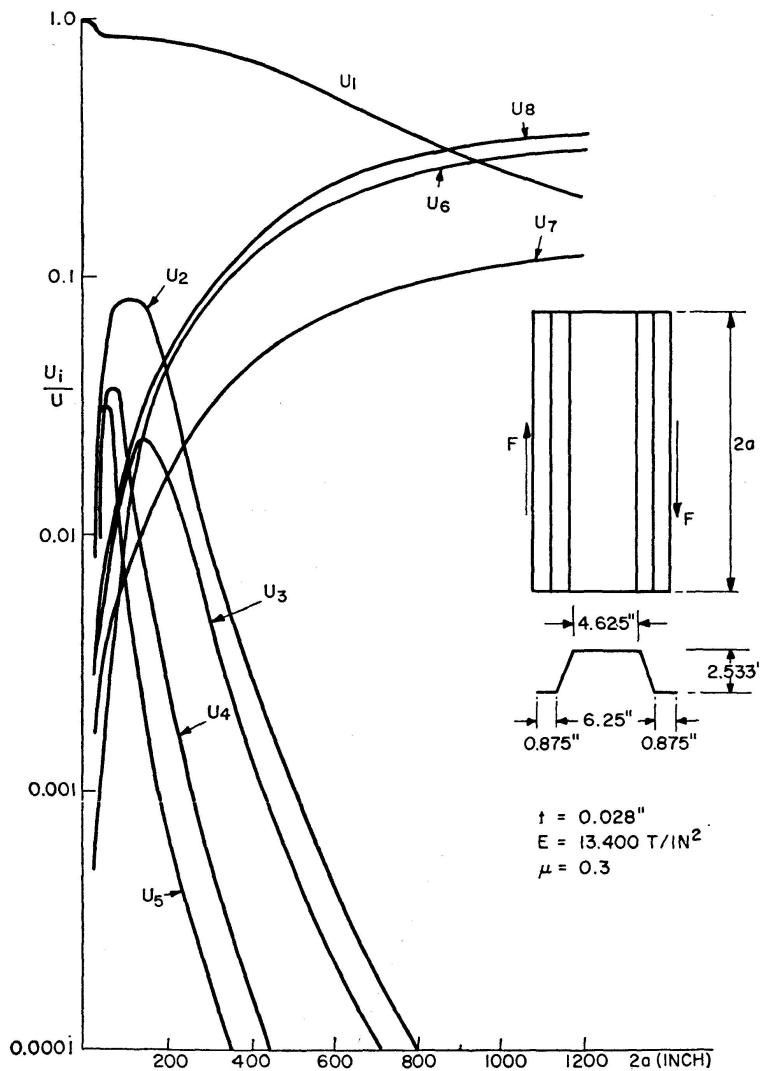


Fig. 6.

u_B for the same panel for different lengths under a shear load of one ton, that at relatively short lengths (e. g. 50 ins) u_T is almost linear, while u_B and u_S are very small compared with u_T . The deflection expressions of Eqs. (1), (2) and (3) may thus be simplified to the form

$$u_T = c_0 y; \quad u_B = u_S = 0.$$

Under this condition, this method of solution agrees with the assumptions made by BRYAN [2] and MCKENZIE [5].

When the length increases, energy terms due to membrane stresses have more effect. Fig. 6 shows that energy terms U_2 , U_3 , U_4 and U_5 first increase in importance with increasing panel length. At the same time (Fig. 11) the top plate acquires a non-linear shape (see u_T for $2a = 100$ in. and 400 in.) and deflections of the side and bottom plates (u_S and u_B) become relatively larger. For long panels (Fig. 6) the influence of energies U_2 , U_3 , U_4 and U_5 again falls due to the decrease in the beam-type bending stiffness of the individual plates. The effect of ignoring these energies is demonstrated in Fig. 7 which shows that their contribution reaches a maximum of 12% of the total energy for a certain panel length.

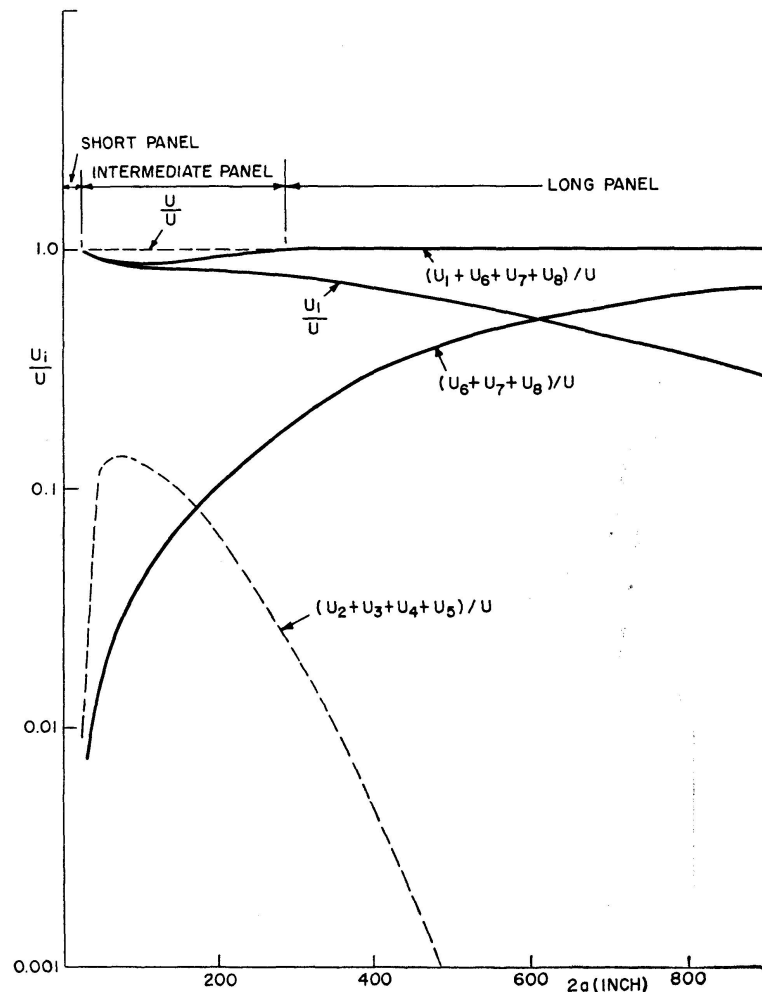


Fig. 7.

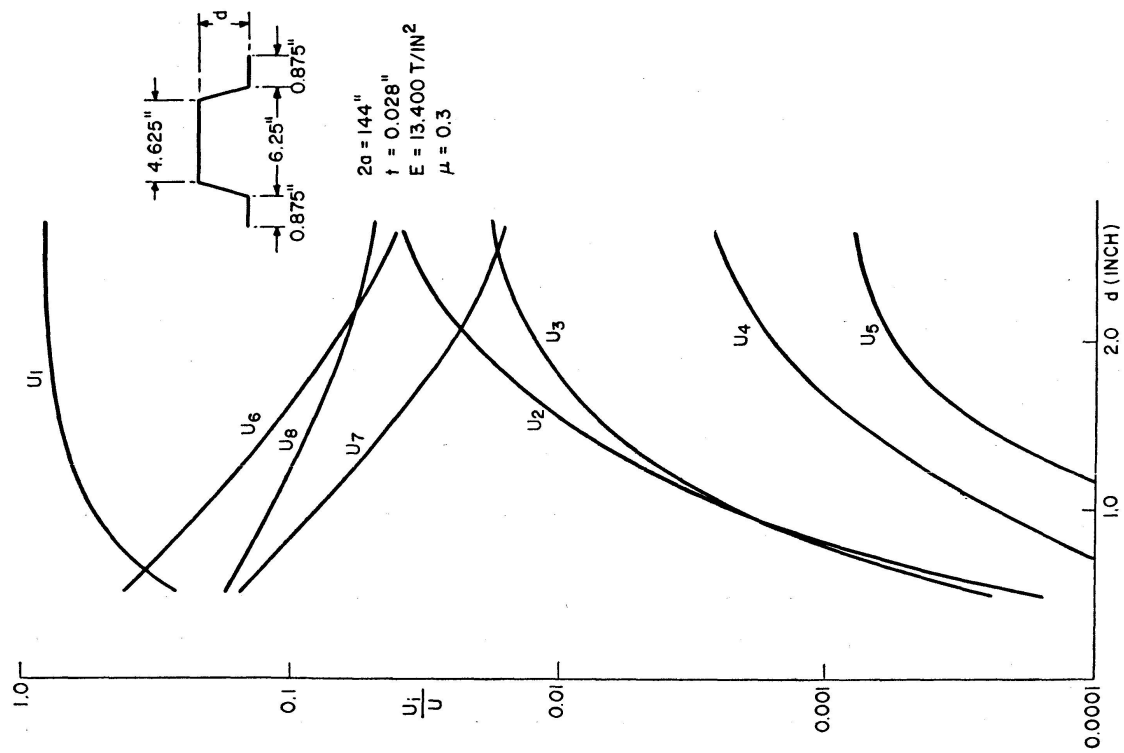


Fig. 8.

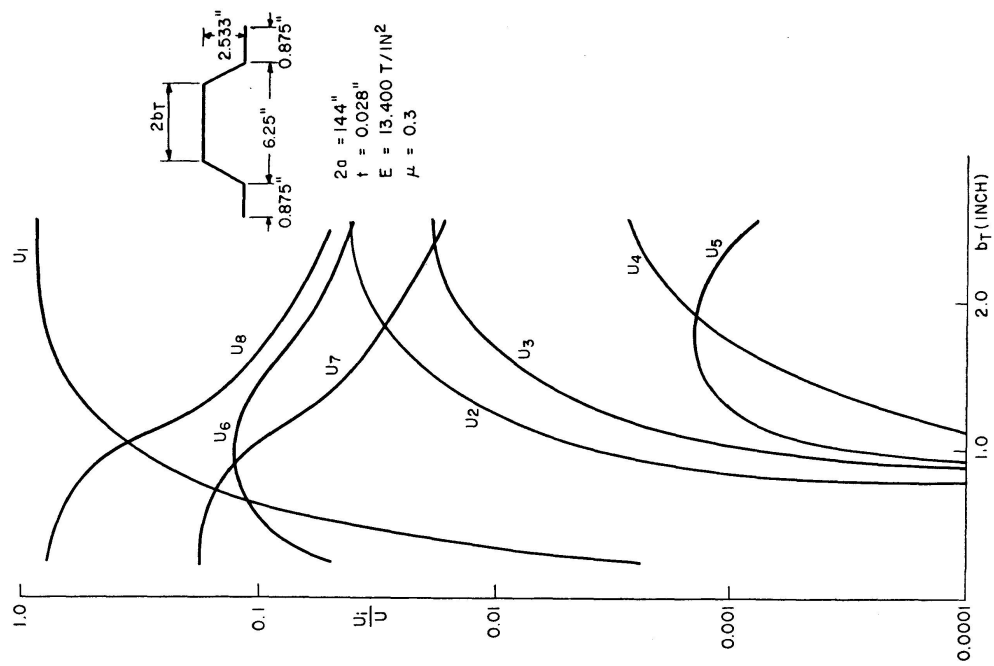


Fig. 9.

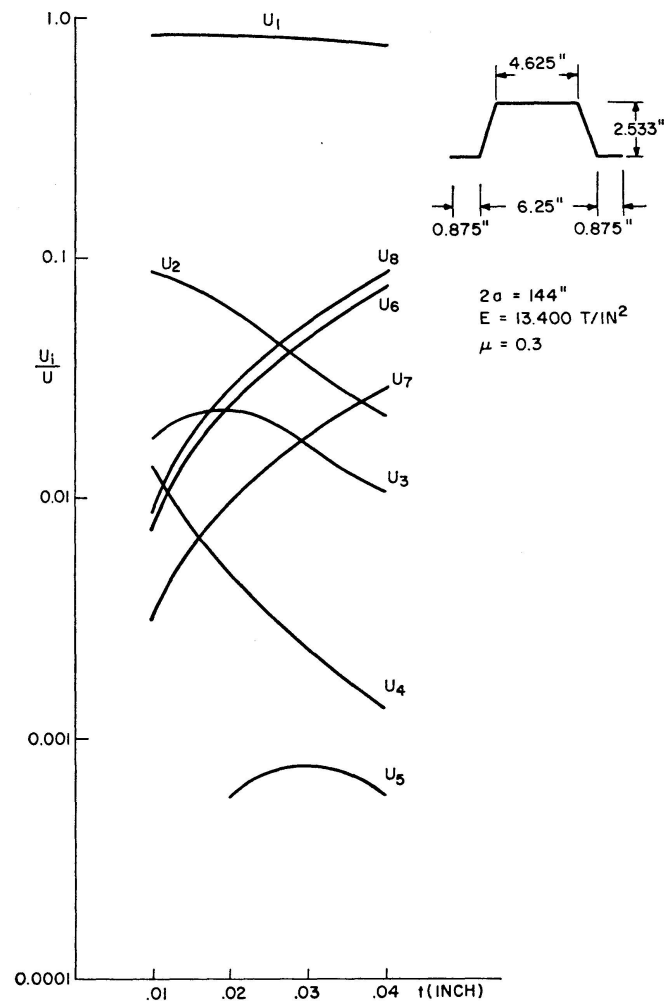


Fig. 10.

When the panel becomes long, the only contributors to the strain energy thus become the “portal frame bending” and the shear strain, and Eq. (54) may be reduced to

$$U = U_1 + U_6 + U_7 + U_8.$$

When the length approaches extremely large values, Fig. 6, U_1 loses importance and the panel behaves in a manner similar to that of a plane plate panel.

In summary, the length of a panel has a great effect on its behaviour as a shear panel. Accordingly, shear panels can be classified, within the practical range, into three different groups depending on their lengths:

1. Short panels, in which the only contribution to their shear deformation is from the “portal frame bending”.
2. Medium length panels, in which all types of stresses included in the analysis result in deformation which contribute significantly to the flexibility of the panel.
3. Long panels, in which the “portal frame bending” and direct shear deformation are the main contributors to panel flexibility.

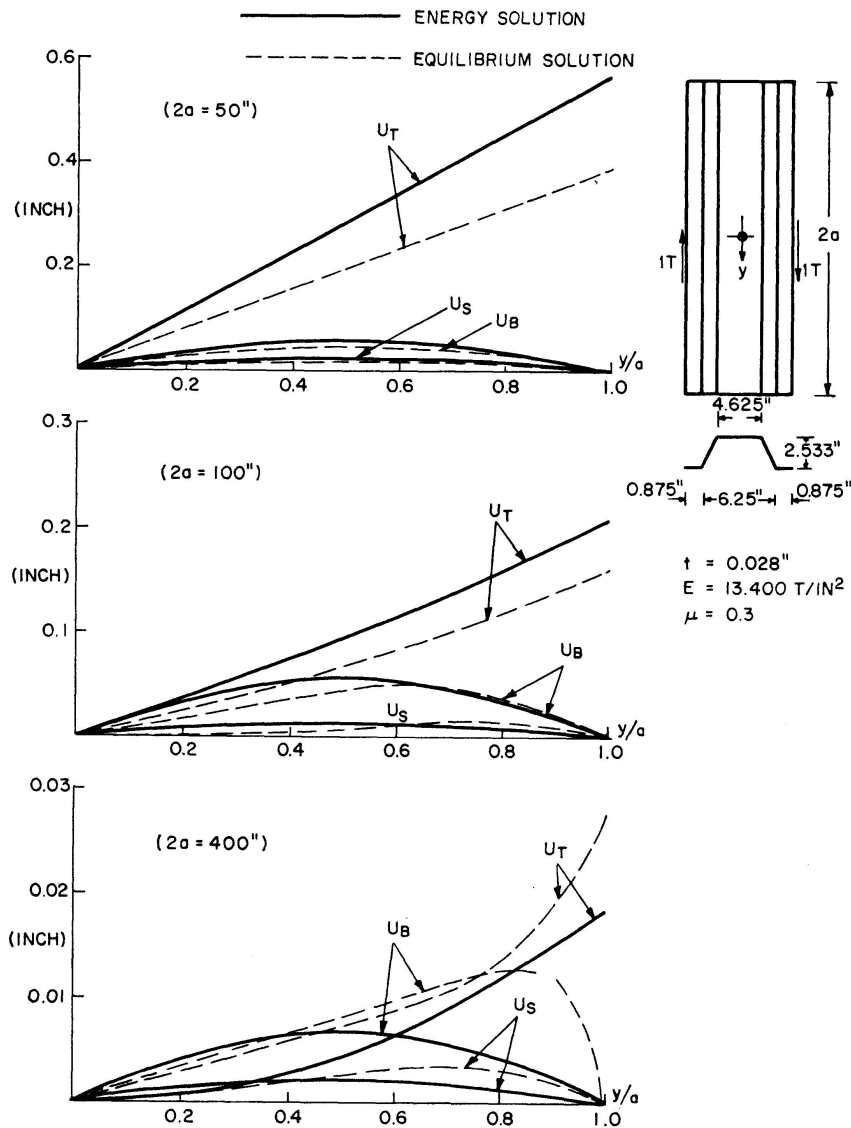


Fig. 11.

Fig. 7 defines, for the particular corrugation, the regions corresponding to the previous grouping. It is to be mentioned, however, that the range of lengths for each region depends also on the panel configuration and the plate thickness.

2. The Effect of the Configuration of the Corrugation

Fig. 8 shows that any increase in the corrugation depth decreases the effect of the energies due to shear strain in the plate and increases the relative contributions of the other energies. Increasing the width of the top plate (Fig. 9) has a similar effect. In general, any change in configuration that increases flexibility in "portal frame bending" has the effect of causing a decrease in the relative importance of direct shear flexibility.

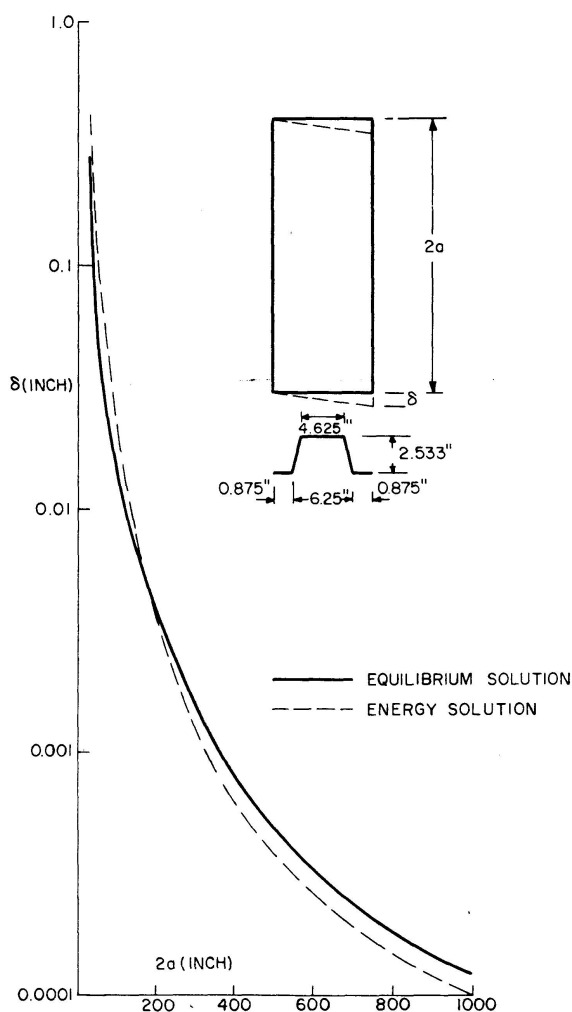


Fig. 12.

3. The Effect of Plate Thickness

The effect of an increase in the plate thickness on the relative importance of energy terms is similar to the effect of increasing the length of the panel (see Fig. 10).

11. Evaluation of the Analysis

Extensive experimental work has been performed [6] to check the presented analysis. Fair agreement has been observed between the analysis and the experimental results for panels of medium lengths. The panels tested having and conditions similar to those assumed in the analysis.

A comparison between results obtained from an equilibrium method [6, 7] and the above energy method is given in Figs. 11 and 12. It is seen from Fig. 12 that the energy method predicts the greater flexibility for short panels. This may be attributed to the neglect of some energy terms among which is the

energy due to torsion of the side plates; this is likely to have a marked effect at short lengths [2]. In case of long panels the energy method predicts stiffer results than the equilibrium method, the reason being that the energy method restricts the deformation of the different plates to the deformation patterns it assumes. The actual deformation, as predicted more closely by the finite difference method (Fig. 11), is in the case of long panels, localized at the ends of the corrugations and diminishes rapidly within the length of the panel.

For medium length panels, Figs. 11 and 12 show that the two methods are in reasonable agreement.

References

1. BRYAN, E. R. and EL-DAKHAKHNI, W. M.: "Shear of corrugated decks: calculated and observed behaviour." *Proc. Instn. Civ. Engrs.*, Vol. 41, Nov. 1968.
2. BRYAN, E. R. and JACKSON, P.: "The shear behaviour of corrugated steel sheeting." *Thin-walled structures Symposium*, University of Swansea, 1967.
3. FALKENBERG, J. C.: Discussion on "Shear flexibility and strength of corrugated decks." *Journal of the Structural Division Proc. A.S.C.E.*, Vol. 95, June, 1969.
4. LUTTRELL, L. D.: "Structural performance of light gauge steel diaphragms." Report No. 319, Department of Structural Engineering, Cornell University, Aug. 1965.
5. MCKENZIE, K. I.: "The shear stiffness of a corrugated web." *Aeronautical Research Council reports and memoranda No. 3342*, London 1963.
6. RASLAN, R. A. S.: "The structural behaviour of corrugated plates." Ph. D. Thesis, University of Manchester, 1969.
7. HORNE, M. R. and RASLAN, R. A. S.: "A finite difference approach to corrugated shear panels" (see below).

Summary

An energy solution is given for the shear rigidity of plates with trapezoidal corrugations retained within rigid edge members connected to the corrugations on one face only of the panel. Allowance is made for the fact that the corrugations twist with a non-linear shape. The relative importance of energy terms due to the various components of membrane and bending stresses is investigated for corrugations of various proportions.

Résumé

On présente une solution par la méthode de l'énergie pour la résistance au cisaillement de tôles à raidisseurs trapézoïdales, qui se trouvent entre des bords rigides et lesquelles sont reliés seulement d'un côté du champ avec les raidisseurs. Les raidisseurs se tordant d'une manière non-linéaire, il y a une tolérance. On analyse aussi pour des raidisseurs à proportions différentes l'importance relative des conditions d'énergie à la suite des différentes composantes dues à la sollicitation de membrane et de flexion.

Zusammenfassung

Es wird eine Energielösung für die Schubsteifigkeit von Blechen mit trapezförmigen Rippen gegeben, die innerhalb starrer Kantenglieder liegt, welche mit den Rippen nur auf einer Seite des Feldes verbunden sind. Eine Toleranz besteht infolge der Tatsache, dass sich die Rippen nach einer nichtlinearen Form verdrehen. Die relative Bedeutung von Energiebedingungen infolge der verschiedenen Komponenten der Membran- und Biegebeanspruchungen wird für Rippen verschiedener Ausmasse untersucht.